Available online at www.sciencedirect.com
SCIENCE DIRECT
Journal of Catalysis 240 (2006) 73–84
JOURNAL OF CATALYSIS
www.elsevier.com/locate/jcat

A comprehensive density functional theory study of ethane dehydrogenation over reduced extra-framework gallium species in ZSM-5 zeolite

Evgeny A. Pidko [a,*], Vladimir B. Kazansky [b], Emiel J.M. Hensen [a], Rutger A. van Santen [a]

[a] *Schuit Institute of Catalysis, Eindhoven University of Technology, PO Box 513, NL-5600 MB Eindhoven, The Netherlands*
[b] *N.D. Zelinsky Institute of Organic Chemistry of Russian Academy of Sciences, Leninsky prospect 47, Moscow, 119991, Russia*

Received 5 December 2005; revised 20 March 2006; accepted 20 March 2006

Abstract

The stability of various gallium species (Ga^+, GaH_2^+, and GaH^{+2}) as models for the active sites in reduced Ga/ZSM-5 and the possible reaction paths of alkane dehydrogenation were studied using a density functional theory cluster modeling approach. In general, alkanes are preferentially activated via an "alkyl" mechanism, in which gallium acts as an acceptor of the alkyl group. A comparison of the computed energetics of the various reaction paths for ethane indicates that the catalytic reaction most likely proceeds over Ga^+. The initial step of C–H activation is the oxidative addition of an alkane molecule to the Ga^+ cation, which proceeds via an indirect heterolytic mechanism involving the basic oxygen atoms of the zeolite lattice. Although the catalytic reaction can also occur over GaH_2^+ and GaH^{+2} sites, these paths are not favored. Decomposition of GaH_2^+ leading to formation of Ga^+ during the catalytic cycle is more favorable than regeneration of these sites. The reactivity of GaH^{+2} ions is strongly dependent on the distance between the stabilizing aluminum-occupied oxygen tetrahedra. In cases of greater Al–Al distances, the stability of the GaH^{+2} species is very low, and it decomposes to Ga^+ and a Brønsted acid site, whereas when Al atoms are located more closely, the charge-compensating GaH^{+2} ions are the most stable and exhibit the lowest activity for the initial C–H bond cleavage reaction.

Keywords: Zeolite; Gallium; ZSM-5; Alkane dehydrogenation; DFT calculations; Oxidative addition

1. Introduction

Gallium- and zinc-exchanged H-ZSM-5 zeolites (Ga/ZSM-5 and Zn/ZSM-5) are known to be effective catalysts for promoting the selective conversion of light alkanes to aromatics [1]. The reaction mechanism is thought to consist of a complex scheme involving dehydrogenation, oligomerization, and ring-closure steps [2–16]. The modifying cations play key roles in dehydrogenation of paraffins [2–5,14–16], whereas Brønsted acid protons catalyze the oligomerization of the olefins thus produced and possibly their subsequent aromatization. Numerous experimental [2–16] and theoretical [17–22] studies have been devoted to investigating the mechanism of catalytic dehydrogenation of light alkanes over gallium-exchanged ZSM-5 zeolites. However, the structure of the active intrazeolite Ga species and, accordingly, the mechanism of hydrocarbon activation have not been fully elucidated.

Extra-framework gallium is introduced into zeolites by either a conventional ion-exchange technique or solid-state ion exchange. In both cases, gallium is initially deposited on the external surface of the zeolite crystals, because hydrated Ga^{+3} ions are too bulky to enter the elliptical channels of ZSM-5 [23]. The Ga_2O_3 species obtained after calcination are reduced during pretreatment with hydrogen or with the hydrocarbon feed to Ga_2O species that migrate into the zeolite channels [11,12]. These mobile species react with the zeolitic Brønsted acid protons, resulting in formation of reduced cationic Ga^+, GaH_2^+, or GaH^{+2} species bound to zeolite oxygen atoms. The resulting material may contain several types of reduced Ga species besides gallium oxide particles if the reduction process is not complete. The oxide species may include bulkier aggregates on the external surface or smaller ones in the micropore space of the zeolite. Meitzner et al. [11] found using in situ Ga K-edge X-ray absorption spectroscopy that in the working catalyst gal-

* Corresponding author. Fax: +31 40 245 5054.
E-mail address: e.a.pidko@tue.nl (E.A. Pidko).

0021-9517/$ – see front matter
doi:10.1016/j.jcat.2006.03.011

lium is present in reduced Ga^+ form, although the oxidation state changes to 3+ on cooling to lower temperatures. Similarly, Kazansky et al. [15] found that Ga^+ species are the most stable species at high temperatures and that oxidative addition of hydrogen to Ga^+ leads to GaH_2^+ species at lower temperatures. It is important to note that these gallium hydride species are relatively stable and decompose only slowly at higher temperatures [15].

Recently, a new and completely anhydrous route for the preparation of well-defined cationic Ga species via chemical vapor deposition of trimethylgallium to anhydrous HZSM-5 has been reported [14–16,24–26]. Careful removal of the methyl ligands by reduction leads to GaH_2^+ cations, which can then be decomposed at high temperatures to Ga^+ cations. When Ga^+ cations are predominant in ZSM-5, stable activity in propane dehydrogenation to propylene is observed [16]. Decreased activity is found when the catalyst contains GaH_2^+ cations. The higher activity at steady state is attributed to the decomposition of less active GaH_2^+ cations to Ga^+ under the reducing high-temperature reaction conditions.

Most theoretical studies have considered GaH_2^+ as the active site for alkane dehydrogenation [17,18,21,22]. Frash and van Santen [17] proposed a three-step mechanism including (i) "alkyl" ($R^{\delta-}$–$H^{\delta+}$) activation of the C–H bond, resulting in the formation of a zeolitic Brønsted acid proton and a rather unstable neutral H_2Ga–R species; (ii) the subsequent desorption of molecular hydrogen via recombination of the acidic proton and one of the hydride ions bounded to gallium; and (iii) the decomposition of the resulting $[H–Ga–R]^+$ complex to alkene and GaH_2^+. The decomposition step is rate-limiting, and an activation energy of 254 kJ/mol is computed for a model reaction of ethane dehydrogenation. Alternatively, a one-step concerted mechanism over GaH_2^+ was recently considered by Pereira and Nascimento [21]. The activation energy for this process is substantially higher (by 90 kJ/mol) than the mechanism proposed by Frash and van Santen [17] and, consequently, this mechanism is less likely. Very recently, Joshi and Thomson [22] proposed the existence of bivalent extra-framework gallium species (GaH^{+2}) close to a pair of tetrahedral framework Al species in ZSM-5 zeolite as active sites for alkane dehydrogenation. The overall activation energy for the "carbenium" pathway for ethane activation over GaH^{+2} species, which are stabilized by two aluminum-containing oxygen tetrahedra, lie in the range of 260–360 kJ/mol, depending on the cation site at which GaH^{+2} species were stabilized. Moreover, the choice for a positively charged alkyl group for the initial activation of ethane contrasts with earlier proposals.

The recent experimental results indicating that Ga^+ cations are the active sites [14–16] led us to reconsider the reaction mechanism of alkane activation over reduced Ga cations stabilized in zeolites. Here we present a detailed comparative analysis of the reactivity of various cationic species (Ga^+, GaH_2^+, and GaH^{+2}) by density functional theory (DFT) cluster calculations. In addition, we discuss the relative stability of the various cationic Ga species and the dependence of their chemical properties on the aluminum distribution in ZSM-5 zeolite.

2. Experimental

Dehydrogenation of ethane over Ga/ZSM-5 zeolite, as well as stability of different gallium-containing active sites, was studied using $GaHAl_2Si_6O_9H_{14}$ and $GaH_3Al_2Si_6O_9H_{14}$ cluster models, which represent two adjacent five rings from the wall of the straight channel of ZSM-5 zeolite. Ga^+, GaH_2^+, and GaH^{+2} cations compensated the negative charge of the $[AlO_2]^-$ unit in one ring, whereas for the first two types of cations, the other negative charge in the other ring was stabilized by a proton. Al atoms were placed in T12 and T8 lattice positions [27] to model a cation site (Z_d) with distantly separated anionic sites, whereas the next nearest T12 and T6 lattice positions were occupied with aluminum atoms in the cluster Z_s. The distance between two aluminum ions was equal to 8.14 Å for the Z_d cluster model and 4.84 Å for the Z_s cluster model. Note that the T12 site is located at the cross-section of the straight and sinusoidal channels of ZSM-5; accordingly, the cations stabilized in the vicinity of this site are considered to have the highest accessibility. Therefore, the charge-compensating gallium species were located in the five-ring-containing aluminum at the T12 position. Hydrogen atoms were used to saturate the dangling Si–O bonds at the periphery of the cluster. The starting geometry of the clusters corresponded to the real lattice of the ZSM-5 zeolite corresponding to X-ray diffraction data [28].

DFT, with the B3LYP [29] hybride exchange-correlation functional, was used to perform all of the calculations. Earlier, the hybride B3LYP method was reported to provide excellent descriptions of various reaction profiles and particularly of geometries, heats of reaction, activation energies, and vibrational properties of various molecules [30]. Geometry optimization and saddlepoint searches were all performed using the Gaussian 03 program [31]. The 6-31G(d,p) basis set was used for the exchanged gallium cation and the bridging hydroxyl group, whereas the ethane molecule and the zeolitic oxygen atoms were described by the 6-311G(d,p) basis set. Al and Si atoms of the zeolite framework, as well as the boundary (H*) hydrogen atoms, were treated by the D95-Dunning/Huzinaga basis set. It was shown earlier that such a compromise is successful for studies of cation-exchanged zeolites [32–34].

As described previously [32–34], special restrictions on the positions of the boundary H* atoms were imposed during the optimization procedure. In short, the structure of the initial zeolite cluster was first constrained to the X-ray diffraction data [28]. Subsequently, only Si–H* and Al–H* bond lengths and the position of the gallium ion were optimized, whereas positions of the other atoms, as well as the directions of the bonds, were fixed according to crystallographic data. The positions of the H* atoms in all subsequent calculations were then fixed, whereas the positions of the remaining atoms of the cluster were optimized. All of the energies obtained from the DFT calculations used for estimating the reaction heats and activation barriers were corrected for the zero-point energy.

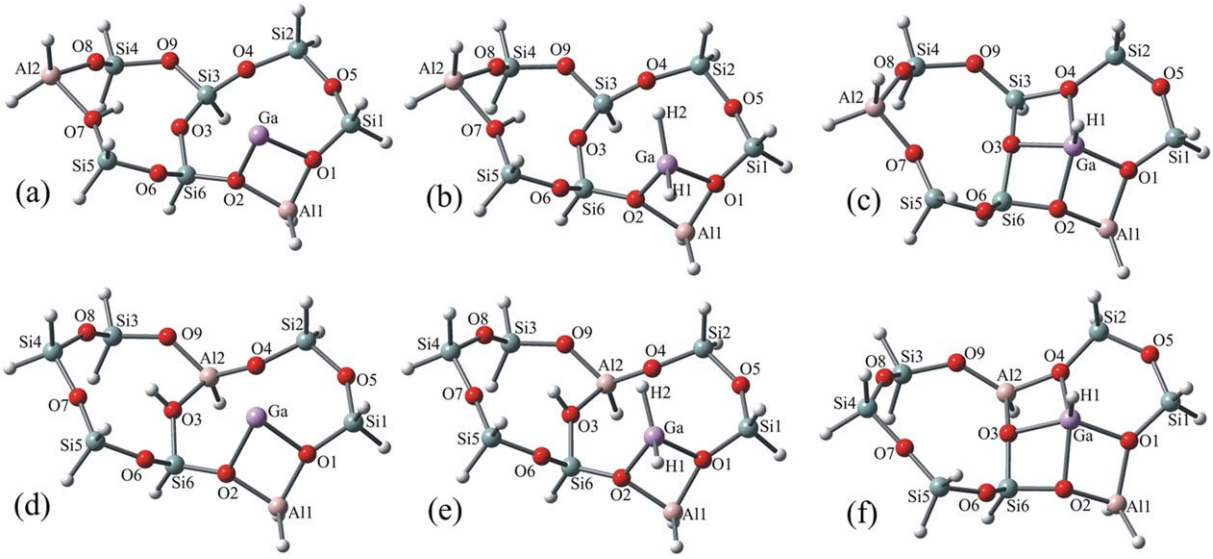

Fig. 1. Optimized structures of (a) Ga Z_d, (b) GaH_2 Z_d, (c) GaH Z_d, (d) Ga Z_s, (e) GaH_2 Z_s, and (f) GaH Z_s clusters.

Table 1
Comparison of the optimized bond lengths and distances (Å), charge parameters (Mulliken charge on atom) and relative energies of Ga^+, GaH_2^+, and GaH^{2+} species stabilized in cluster model with distantly separated Al atoms (Z_d) and with Al atoms located at the next nearest positions (Z_s)

	Ga Z_d	GaH_2 Z_d	GaH Z_d	Ga Z_s	GaH_2 Z_s	GaH Z_s	Zn Z_d[a]	Zn 5T[b]
ΔE (kJ/mol)	0	−24[c]	+88	−105	−115[c]	−207	–	–
Distance								
Ga–O1	2.123	2.011	1.949	2.098	2.000	1.977	1.916	1.961
Ga–O2	2.130	2.014	1.976	2.192	2.045	2.066	1.973	2.058
Ga–O3	3.792	3.840	2.080	3.349	3.713	2.025	2.081	2.058
Ga–O4	3.802	3.987	2.138	2.937	3.692	2.028	2.019	1.961
Ga–H1	–	1.562	1.540	–	1.566	1.549	–	–
Ga–H2	–	1.564	–	–	1.559	–	–	–
Charges on								
Ga	0.548	0.632	0.896	0.525	0.622	0.863	0.984	–
O1	−1.126	−1.128	−1.123	−1.130	−1.128	−1.115	−1.138	–
O2	−1.142	−1.147	−1.100	−1.128	−1.130	−1.098	−1.149	–
O3	−1.127	−1.125	−1.116	−0.968	−0.951	−1.127	−1.149	–
O4	−1.086	−1.083	−1.126	−1.144	−1.142	−1.144	−1.139	–
H1	–	−0.079	0.036	–	−0.082	0.014		–
H2	–	−0.080	–	–	−0.067	–		–

[a] The geometry and charge parameters for ZnZ_d model were obtained from Ref. [32].
[b] The geometry parameters for Zn ion stabilized at 5T zeolitic ring with next-nearest Al atoms were obtained from Ref. [35].
[c] ΔE for reaction $Ga^+Z^- + H_2 \rightarrow GaH_2^+Z^-$.

3. Results

3.1. Structure and properties of active sites

Fig. 1 displays the optimized structures of Ga^+, GaH_2^+, and GaH^{+2} ions stabilized in the Z_d (distantly separated Al ions) and Z_s (Al ions in the next-nearest positions). Table 1 lists the corresponding optimized Ga–O and Ga–H bond lengths, the atomic charges, and the relative energies. The univalent cations Ga^+ and GaH_2^+ are located in close vicinity to one of aluminum atoms (T12) and coordinate to two adjacent oxygen atoms (O1 and O2). The structural parameters show that the Ga–O bonds (Ga–O1 and Ga–O2) between Ga and lattice oxygens are somewhat shorter for the dihydrido-gallyl ion than for the Ga^+ cation. On the other hand, the Ga–O distances to the other oxygens (Ga–O3 and Ga–O4) of the cluster are shorter in the latter case. This is most likely due to the repulsive interactions of basic oxygen atoms of the zeolite framework with the negatively charged hydride ions in the bonded GaH_2^+ complex. On the other hand, weak electrostatic interaction of Ga^+ ion with remote zeolitic oxygens leads to additional stabilization of the cation. This is also supported by the fact that the increased basicity of O3 and O4 atoms due to exchange of the Si by Al atom at framework T6 position results in a significant decrease of the corresponding Ga–O distances in the Ga Z_s cluster. The computed Ga–O and Ga–H distances for GaH_2^+ species stabilized in either Z_d or Z_s clusters agree very well with those reported for the dihydrido-gallyl ion in the extended cluster model containing 11 T atoms [22], corresponding to the cation site located at the cross-section of the straight and sinu-

soidal channels of ZSM-5 zeolite. We infer that the presence of an additional anionic site in our model that is balanced by an acidic proton does not significantly affect the properties of the gallium-containing sites (Ga^+ and $GaH_2{}^+$).

The bivalent GaH^{+2} ion is preferentially located at the Z_d site (Fig. 1c) near the Al1 atom and at a rather long distance [r(Ga–Al2) = 6.857 Å] from the second anionic site of the cluster. Table 1 shows that the GaH^{+2} ion is coordinated by four oxygen atoms, two of which are bonded at a somewhat shorter distance (∼0.2 Å) due to the lower basicity of the oxygen atoms of the silicon-occupied oxygen tetrahedra compared with those of the aluminum-occupied tetrahedra. This is in agreement with the fact that the GaH^{+2} ion sits almost in the center (Ga–Al1 and Ga–Al2 distances are equal to 2.995 and 2.957 Å, respectively) of the 5T rings containing two anionic sites (GaH Z_s structure; Fig. 1f).

The Lewis acidic properties of the GaH^{+2} ions should be similar to those of Zn^{+2}, and, accordingly, we would expect similar bonding properties of these charge-compensating ions with the zeolite. Indeed, the Zn–O bond lengths (Table 1) reported by Zhidomirov et al. [32–34] for zinc stabilized at the similar cationic site cohere well with the geometry parameters of the GaH Z_d cluster, taking into account the slightly smaller radius of the Ga^{3+} cation. The geometry of the GaH Z_s correlates also very well with that reported by Shubin et al. [35] for zinc ions stabilized in the 5T zeolitic ring containing two aluminum atoms (Table 1). Therefore, one expects the GaH^{+2} ions to exhibit similar chemical properties to those of exchanged zinc ions.

Desorption of H_2 from $GaH_2{}^+$ (1) resulting in formation of Ga^+ ions is slightly endothermic (Table 1). However, due to increase of entropy at high temperature, the equilibrium of this process is shifted strongly toward Ga^+ formation ($\Delta G^\circ_{823\ K} = -75$ and -101 kJ/mol, respectively, for Z_d and Z_s models). This finding corresponds well to the experimental observation that charge-compensating Ga^+ ions are transformed into dihydrido-gallyl ions only at lower temperatures in hydrogen atmosphere [11,15]. Dehydrogenation of these species, resulting in formation of univalent gallium ions, was found to proceed on high-temperature treatment in inert atmosphere or in vacuum [15],

$$GaH_2{}^+Z^- \rightleftarrows Ga^+Z^- + H_2. \quad (1)$$

Formation of GaH^{+2} ions from Ga^+ and a Brønsted acid proton (2) is found to be a strongly endothermic process ($\Delta E = +88$ kJ/mol) for the case of a long Al–Al distance (Z_d mode) and a strongly exothermic process ($\Delta E = -102$ kJ/mol) when two Al atoms are placed at the next-nearest positions of the cation site (Table 1),

$$Ga^+Z^- + H^+Z^- \rightleftarrows Z^- + GaH^{+2}Z^-. \quad (2)$$

Therefore, we predict that for relatively long Al–Al distances, the equilibrium of reaction (2) shifts to the side of the univalent Ga^+ ion and the proton. On the other hand, when located in the vicinity of two anionic sites, the bivalent GaH^{+2} ion is more stable (by 102 kJ/mol) than the Ga^+ Z_s site (Table 1), and the equilibrium will shift to the formation of the gallium monohydride.

3.2. Ethane dehydrogenation over Ga^+

In agreement with recent experimental DRIFTS investigations [14], molecular adsorption of ethane on Ga Z_d does not result in any specific interaction between C_2H_6 and the adsorption site at low temperature. The geometry and charge properties of both the C_2H_6 moiety and the cluster model in the adsorption complex are similar to those calculated for the individual fragments. Recent experiments [15] indicate that at moderate temperature (523 K), dehydrogenation of ethane over Ga/ZSM-5 zeolite is initiated by dissociative adsorption of C_2H_6 on charge-compensating reduced Ga^+ species, resulting in the formation of gallium-ethyl hydride according to

$$Ga^+Z^- + C_2H_6 \rightarrow [H\text{–}Ga\text{–}C_2H_5]^+Z^-. \quad (3)$$

Reaction (3) as written corresponds to an oxidative addition of ethane to Ga^+, resulting in oxidation of the univalent gallium to Ga^{+3}. The activation energy of the direct homolytic cleavage of the C–H bond of an ethane molecule on the Ga Z_d cluster is computed as 374 kJ/mol [Fig. 2, route (a), **TS1′**]. This barrier is too high to explain the experimentally observed formation of $[C_2H_5\text{–}Ga\text{–}H]^+$ species (**II**) at 523 K. Moreover, the value for the activation energy is very close to the C–H bond energy in molecular ethane (423 kJ/mol [36]). Thus, it appears that for the case of ethane activation over Ga^+-exchanged ZSM-5, stabilization of the nonpolar transition state (**TS1′**) is very weak, and most likely the role of the active site is limited to stabilize the products of the homolytic dissociation of ethane via chemisorption of C_2H_5 and H radicals.

Generally, alkanes are activated over transition metal complexes [37–39] via formation of a σ-C_2H_6 complex. The bonding of a hydrocarbon molecule with the transition metal ion in such complexes is described by a synergetic combination of the ligand-to-metal donation from the σ C–H orbitals of the hydrocarbon to the partially occupied s-orbital of the transition metal (TM) and the metal-to-ligand back-donation from the d_π orbital to the C–H σ^*-orbitals. Such interactions result in a very strong weakening of the C–H bond, which in turn, together with formation of new TM…C and TM…H bonds, significantly facilitates homolytic C–H bond cleavage. However, the fully occupied 3d-orbitals of univalent gallium are of too-low energy and thus do not contribute to the backdonation. Moreover, because the 4s-orbital is occupied, it will not act effectively as an electron-acceptor orbital. Thus, the formation of the σ CH complex between ethane and Ga^+ is unlikely, and, correspondingly, the energy cost for the homolytic dissociation of ethane over Ga Z_d is very close to that for the gas-phase dissociation.

Alternatively, the interaction with a soft Lewis acid–base pair consisting of Ga^+ and the basic oxygen atom of the zeolite lattice appears to be responsible for the initial C–H bond cleavage. This route of heterolytic activation of the C–H bond is shown in Fig. 2, route (b). The geometry and charge parameters of the intermediates and transition-state structures are summarized in Table 2. In the initial step, heterolytic dissociation of the

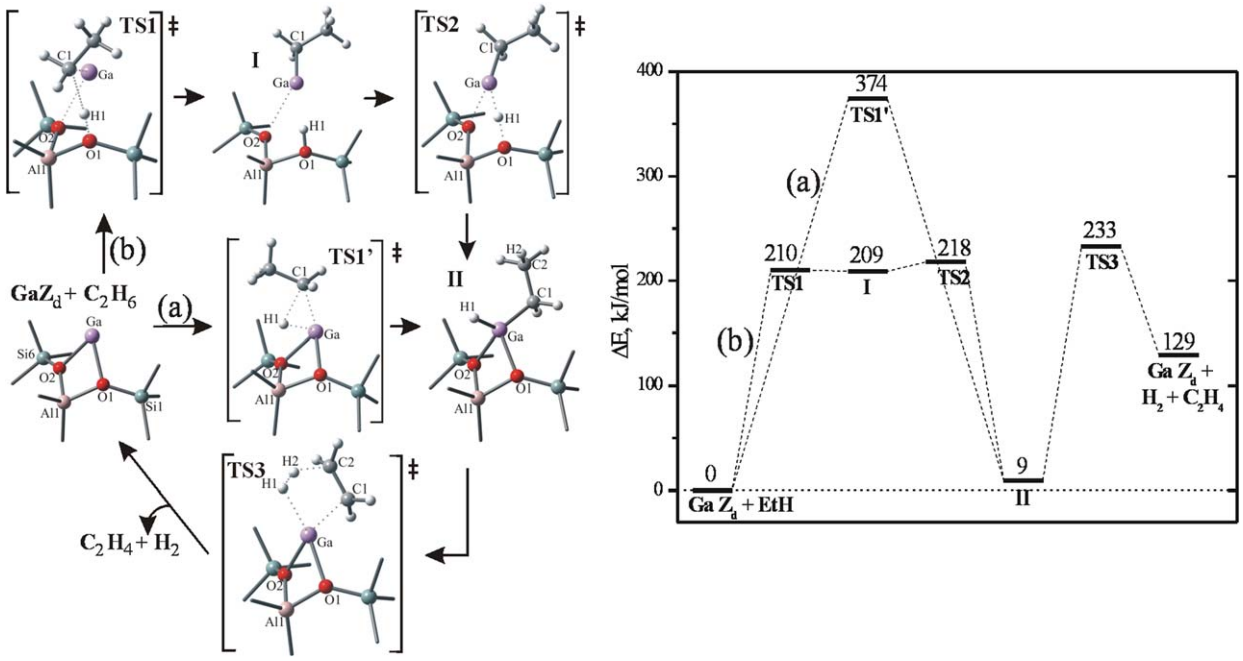

Fig. 2. Homolytic (a) and heterolytic (b) "alkyl" pathways of ethane dehydrogenation over Ga Z_d site.

Table 2
Optimized bond lengths (Å), charges parameters (Mulliken charge on atom) of the intermediates along homolytic and heterolytic reaction paths on Ga Z_d site

	Ga Z_d + C_2H_6[a]	TS1′	TS1	I	TS2	II	TS3
Distance							
Ga–O1	2.123	2.030	3.060	3.188	2.848	2.029	2.130
Ga–O2	2.130	2.047	2.421	2.897	2.227	2.039	2.135
Ga–C1	–	2.204	2.226	2.041	2.017	1.984	2.280
Ga–H1	–	1.804	2.426	2.289	1.792	1.569	1.993
O1–H1	–	–	1.037	1.007	1.257	–	–
C1–H1	1.094	1.834	1.757	–	–	–	–
C2–H2	–	–	–	–	–	1.094	1.604
H1–H2	–	–	–	–	–	3.361	0.871
Charges on							
Ga	0.548	0.341	0.282	0.187	0.262	0.700	0.592
O1	−1.126	−1.106	−0.992	−0.928	−1.028	−1.125	−1.099
O2	−1.142	−1.138	−1.156	−1.142	−1.142	−1.145	−1.047
C1	−0.317	−0.327	−0.639	−0.449	−0.432	−0.457	−0.417
H1	0.106	−0.063	0.461	0.378	0.338	−0.075	−0.032
C2	–	–	–	–	–	−0.284	−0.261
H2	–	–	–	–	–	0.111	0.051

[a] For isolated C_2H_6 molecule distances and charges were computed at B3LYP DFT level with 6-311G(d,p). For isolated C_2H_4 molecule Mulliken charges computed at the same level are −0.219 and 0.109 on C and H atoms, respectively.

C–H bond results in formation of a neutral Ga–C_2H_5 species in the vicinity of a zeolitic Brønsted acid site (**I**). The calculated activation energy (**TS1**, 210 kJ/mol) is significantly lower than that obtained for the homolytic path. The corresponding transition state structure (**TS1**) is characterized by very strong polarization of the reacting C–H bond following the "alkyl" mechanism; that is, both the positive charge on the H atom and the negative charge on carbon strongly increase compared with gas-phase C_2H_6. At the same time, the positive charge on the gallium decreases, indicating weakening bonds between the cation and zeolitic oxygen. The partial negative charge on the O1 atom also decreases due to bonding with the proton from ethane. Similar effects were also observed for the O3 atom of the Z_s cluster model (Table 1) for the Ga Z_s and GaH_2 Z_s clusters.

The intermediate (**I**) resulting from heterolytic activation of ethane over the Ga Z_d site is very unstable and readily rearranges to the stable product (**II**). This reaction proceeds via oxidation of the Ga–C_2H_5 species by the Brønsted acid site with a very low activation barrier (9 kJ/mol, **TS2**). The ease of formation of complex (**II**) also explains why only the product of oxidative addition was observed experimentally [15].

The final step in ethane dehydrogenation over Ga^+ was found to be a one-step desorption of H_2 and C_2H_4 molecules via the **TS3** structure. This reaction can be described as a "destructive reductive elimination," resulting in reduction of the Ga^{+3}

ion and regeneration of the initial Ga Z_d site. Table 2 shows that the hydrogen atoms of the free methyl group in structure **II** are positively charged, whereas the H atom bounded to gallium is negatively charged. Hence, the catalytic cycle is closed by the recombination of these atoms to form molecular hydrogen via transition state **TS3**. The activation barrier of the latter process is computed as 224 kJ/mol. This value is slightly higher than that calculated for the initial C–H cleavage (210 kJ/mol). The overall activation energy of the ethane dehydrogenation over the reduced dehydrogenated Ga/ZSM-5 zeolite is 233 kJ/mol.

3.3. Ethane activation over GaH_2^+

To compare the reactivities of the various charge-compensating gallium species, we investigated the alkyl activation pathway over the GaH_2^+ site proposed by Frash and van Santen [17] with the present Z_d cluster model. The energetics for this mechanism are presented in Fig. 3, and the geometry and charge parameters of the intermediates and transition-state structures are listed in Table 3.

Similar to the findings for Ga^+, molecular adsorption of ethane on the dihydrido-gallyl ion stabilized in the Z_d cluster was very weak and did not result in any significant perturbation of either the adsorbed molecule or the adsorption site. Thus, it is assumed that this molecular adsorption does not influence the subsequent chemical activation of C_2H_6 molecules. The mechanism of the initial activation of the hydrocarbon molecule on dihydrido-gallyl ion is very similar to that suggested for the heterolytic dissociation of ethane on Ga Z_d. Indeed, a very strong polarization of the reacting C–H bond is observed in the **TS4** structure, leading to heterolytic C–H bond splitting with formation of a neutral $(H^-)_2Ga^{+3}$–$C_2H_5^-$ species in the vicinity of a Brønsted acid site (**III**). The calculated activation energy for this elementary step (193 kJ/mol) is significantly higher than that (158 kJ/mol) reported previously [17] for GaH_2^+ species stabilized in a fully optimized 3T cluster. On the other hand, the present value is slightly lower than that (203 kJ/mol) reported by Yoshi and Thomson [22] for the dihydrido-gallyl ion stabilized at a more extended cluster model containing 11T atoms. We attribute the higher activation barrier than that reported by Frash and van Santen [17] mainly to greater steric hindrance of the interaction of the C–H bond with the Ga…O pair caused by the constrained geometry and the larger size of the cluster model. The difference between the present result and that reported in [22] is also attributed to the steric factors and to different basic properties of the zeolitic O atom involved in the C–H activation resulting from size differences of the cluster model.

The H_2Ga–C_2H_6 species formed in the initial step are stabilized by interaction between a hydride ion (H1′) bonded to the gallium and an acidic proton (H1). This interaction results in a strong elongation (by about 0.2 Å) of the O1–H1 bond. The Ga–O2 distance in structure **III** (Table 3) is significantly less than the corresponding distance in structure **I** (Table 2) and is indicative of the stronger interaction of the trivalent gallium in the H_2Ga–C_2H_6 species with the framework zeolitic oxygens. Due to the latter interaction, the coordination of the Ga^{+3} ion in structure **III** is rather close to tetrahedral, which is known to be preferred for Ga^{+3}-containing compounds [40]. Thus, both attractive interactions provide additional stabilization of the reactive species **III** compared with Ga–C_2H_6 species (**I**). Moreover, this facilitates subsequent decomposition of **III** via desorption of H_2 and formation of the stable tetrahedral gallium in the $[H–Ga–C_2H_5]^+$ ion (**II**). The calculated activation barrier (**TS5**) for this process is equal to 2 kJ/mol.

To close the catalytic cycle via regeneration of the initial dihydrido-gallyl ion, the decomposition of the structure **II** was proposed by Frash and van Santen to proceed via abstraction of a hydride ion from the β-position of the ethyl group by the positively charged gallium atom and simultaneous desorption of ethylene [Fig. 3, route (a)]. The activation energy for this process was 257 kJ/mol, in an excellent agreement with the previously reported values of 258 kJ/mol [22] and 254 kJ/mol [17]. This close agreement indicates that the chemical properties of the exchanged trivalent gallium species almost do not depend on the surrounding unless the other atoms of the zeolite are involved in the reaction. However, Table 3 shows that both the abstracting H atom of the β-methyl group and the gallium ion are positively charged. Thus, regeneration of the GaH_2^+ active site requires "repolarization" of the C–H bond, a process that appears to be unfavorable. On the other hand, simultaneous desorption of H_2 and C_2H_4 [Fig. 3, route (b)], which results in formation of the univalent gallium ion (Ga Z_d), is about 30 kJ/mol more favorable than closure of the cycle with regeneration of the dihydrido-gallyl ion. Note that this process is also strongly favored because of the entropy factor. The calculated Gibbs energy changes (ΔG°_{823}) at the conditions of catalytic reaction (823 K, 1 atm.) are equal to +1 for route (a) and −74 kJ/mol for route (b).

3.4. Ethane activation over GaH^{+2}

Recently, Joshi and Thomson [22] proposed that the GaH^{+2} species stabilized in the vicinity of two framework Al atoms are the active species for hydrocarbon dehydrogenation in Ga/ZSM-5 catalysts. The initial step of alkane activation over these active sites was suggested to be a heterolytic dissociation of the C–H bond via a "carbenium" mechanism, resulting in formation of a "carbenium" ion attached to the basic oxygen of the zeolite and a hydride ion bonded to gallium (GaH Z_d + C_2H_6 → V) [Fig. 4, route (a)]. In view of earlier results [17,41], this mechanism seems disputable. Thus, to clarify the mechanism of alkane activation over GaH^{+2} species and to compare the reactivity with those of the earlier discussed gallium containing sites, the initial activation of ethane over GaH^{+2} stabilized at the Z_d cluster was computed.

The elementary steps and the reaction energy diagrams for the "carbenium" and "alkyl" pathways of ethane activation over GaH Z_d cluster are shown in Fig. 4, routes (a) and (b), respectively. The geometry and charge parameters of the intermediates and transition state structures involved are summarized in Table 4. According to Joshi and Thomson [22], activated molecular adsorption of ethane on GaH^{+2} species (structure **IV** in Fig. 4) precedes C–H bond cleavage. In contrast to the

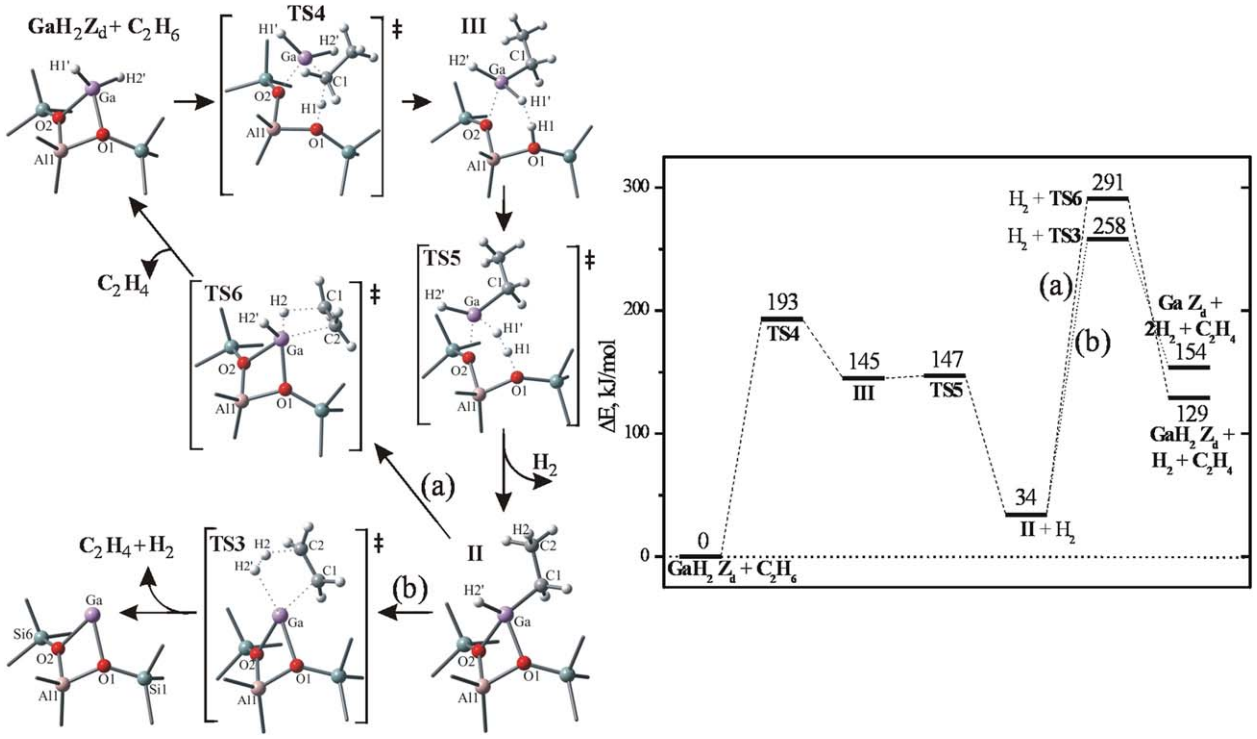

Fig. 3. Reaction paths for the "alkyl activation" mechanism of ethane dehydrogenation (a) over GaH_2 Z_d and dehydrogenation of these species in the catalytic cycle (b) resulting in formation of Ga Z_d.

Table 3
Optimized bond lengths (Å), charges parameters (Mulliken charge on atom) of the intermediates along ethane dehydrogenation reaction paths on GaH_2 Z_d site

	GaH_2 Z_d + C_2H_6	**TS4**	**III**	**TS5**	**II**	**TS6**	**TS3**
Distance							
Ga–O1	2.011	3.029	3.226	3.181	2.029	2.034	2.130
Ga–O2	2.014	2.090	2.196	2.098	2.039	2.159	2.135
Ga–H1′	1.562	1.569	1.660	1.757	–	–	–
Ga–H2′	1.564	1.573	1.576	1.570	1.569	1.554	1.993
Ga–C1	–	2.200	2.005	1.997	1.984	2.234	2.280
O1–H1	–	1.189	1.037	1.237	–	–	–
C1–H1	1.094	1.490	–	–	–	–	–
H1′–H1	–	3.383	1.267	0.972	–	–	–
C2–H2	–	–	–	–	1.094	1.681	1.604
Ga–H2	–	–	–	–	3.134	1.674	–
H2′–H2	–	–	–	–	3.361	–	0.871
Charges on							
Ga	0.632	0.381	0.454	0.514	0.700	0.587	0.592
O1	−1.128	−1.078	−0.978	−1.076	−1.125	−1.127	−1.099
O2	−1.147	−1.154	−1.154	−1.144	−1.145	−1.155	−1.047
H1′	−0.079	−0.104	−0.165	−0.133	–	–	–
H2′	−0.080	−0.101	−0.125	−0.100	−0.075	−0.034	−0.032
C1	−0.317	−0.547	−0.443	−0.433	−0.457	−0.402	−0.417
H1	0.106	0.473	0.339	0.305	–	–	–
C2	–	–	–	–	−0.284	−0.184	−0.261
H2	–	–	–	–	0.111	−0.091	0.051

aforementioned molecular adsorption of C_2H_6 on Ga Z_d and GaH_2 Z_d, this process leads to very significant changes in the geometry and charge parameters of both adsorbed C_2H_6 and the adsorption site. The Ga–O coordination opens (Ga–O3 and Ga–O4 bonds are broken), and the GaH^{+2} ion partially leaves the cation site (5T ring), so that gallium becomes coordinated to only two framework oxygens (O1 and O2). The coordinative unsaturation of the GaH^{+2} species is then partially compensated by interaction with one of the methyl group of ethane. Formation of such an activated adsorption complex is a strongly endothermic process (GaH Z_d + C_2H_6 → **IV**, ΔE = +68 kJ/mol; Fig. 4), because it requires destruction of a stable fourfold coordination of GaH by the lattice oxygen atoms. On the other hand, coordination of ethane to the cation does not

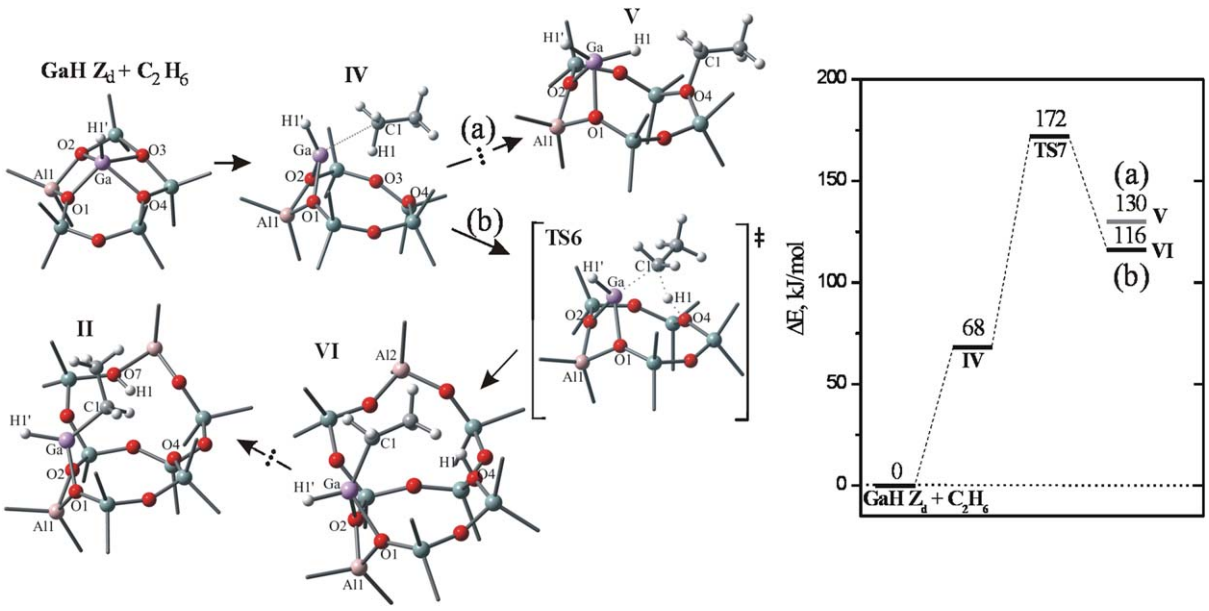

Fig. 4. "Alkyl" (a) and "carbenium" (b) activation of ethane over GaH Z_d.

Table 4
Optimized bond lengths (Å), charges parameters (Mulliken charge on atom) of the intermediates involved in the initial activation of ethane on GaH Z_d site

	GaH_2 Z_d + C_2H_6	**IV**	**V**	**TS6**	**VI**
Distance					
Ga–O1	1.949	1.948	2.058	2.000	2.112
Ga–O2	1.976	1.872	1.979	1.924	1.992
Ga–O3	2.080	3.470	3.615	3.400	3.722
Ga–O4	2.138	3.882	4.372	3.349	4.538
Ga–H1′	1.540	1.533	1.552	1.552	1.559
Ga–C1	–	2.566	–	2.145	1.997
Ga–H1	–	2.027	1.571	2.371	–
O4–C1	–	3.295	1.543	2.664	–
O4–H1	–	2.418	–	1.201	0.980
C1–H1	1.094	1.132	3.172	1.505	3.441
Charge on					
Ga	0.896	0.781	0.638	0.682	0.635
O1	−1.123	−1.107	−1.117	−1.128	−1.119
O2	−1.100	−1.105	−1.149	−1.141	−1.148
O3	−1.116	−1.160	−1.142	−1.161	−1.139
O4	−1.126	−1.126	−0.954	−1.074	−0.916
H1′	0.036	0.057	−0.009	0.021	−0.002
C1	−0.317	−0.411	−0.069	−0.651	−0.413
H1	0.106	0.218	−0.154	0.527	0.408

compensate for the energy loss associated with the breaking of two Ga–O bonds (Ga–O3 and Ga–O4). In other words, it is not possible to form a strong adsorption complex of ethane with GaH Z_d without decreasing the effective coordination number of the cation to the basic zeolitic oxygens, as was observed for Zn^{+2} ion stabilized in a similar cluster model [32,33]. The difference with GaH^{+2} is that the gallium ion in the initial GaH Z_d model is shielded by the attached hydride ion, which hinders the stabilizing charge donation from ethane to the cation. The twofold coordination of GaH^{+2} ion in structure **IV** removes these hindrances. The effective transfer of electron density from ethane to the adsorption site is $0.283e^-$, which is in agreement with the significant decrease in the positive charge of the

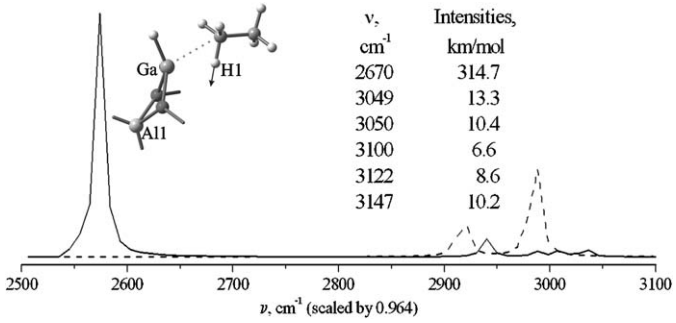

Fig. 5. Calculated IR frequencies of C–H stretching vibrations with their intensities and simulated IR spectrum (with all DFT computed vibrational frequencies scaled by factor 0.964) for structure **IV**. The shape of the C–H vibration mostly perturbed due to interaction with GaH^{+2} ion is shown by "balls and sticks" model. IR spectrum of free C_2H_6 molecule calculated at B3LYP/6-311G(d,p) level is presented for comparison by the dashed line.

GaH^{+2} ion (Table 4). This indicates appreciable Lewis acidity of the "activated" GaH^{+2} ion in a cationic position with distantly placed aluminum ions. The charge transfer is much larger (by $0.168e^-$) than that for ethane adsorption on zinc ions [32], indicating a much stronger Lewis acidity of low-coordinated GaH^{+2} species.

Interaction of the hydrocarbon molecule with the excessively charged low-coordinated monohydrido-gallyl ion results in very strong polarization of the adsorbed molecule. This is reflected in a very strong increase in the negative charge on the carbon atom (C1) and, at the same time, of the positive charge on the hydrogen atom (H1) involved in the interaction (Table 4). In addition, the C1–H1 bond length is 0.038 Å longer than that of the corresponding value for gas-phase ethane. These perturbations of the adsorbed molecule affect the vibrational properties of the C_2H_6 moiety in structure **IV** (Fig. 5). One can see that the calculated IR spectrum of C–H vibrations of **IV** contains five slightly perturbed bands with frequencies close to those observed in the gas phase, whereas one band is very

Table 5
Energetics of initial activation of ethane over Ga^+ and GaH^{+2} sites based on Ga Z_s and GaH Z_s models, respectively

	E_{act} (kJ/mol)	ΔE (kJ/mol)
Ga Z_s		
"Homolytic" path		
$Ga^+Z^- + C_2H_6 \rightarrow [H–Ga–C_2H_5]^+Z^-$	+386	+23
"Heterolytic" path		
$Ga^+Z^- + C_2H_6 \rightarrow Ga–C_2H_5\ldots H^+Z^-$	+219	+194
$Ga–C_2H_5\ldots H^+Z^- \rightarrow [H–Ga–C_2H_5]^+Z^-$	–	−171
GaH Z_s		
"Alkyl" path		
$Z^-GaH^{+2}Z^- + C_2H_6 \rightarrow [H–Ga–C_2H_5]^+Z^- + H^+Z^-$	+252	+125
"Carbenium" path		
$Z^-GaH^{+2}Z^- + C_2H_6 \rightarrow [H–Ga–H]^+Z^- + C_2H_5{}^+Z^-$	–	+274

strongly red-shifted (by >300 cm^{-1}) and exhibits a very high relative intensity compared with those of the other C–H stretching bands. This band corresponds mainly to displacement of the hydrogen atom (H1) for the C1–H1 bond directly interacting with the GaH^{+2} ion. Recently we reported that such a strong perturbation of adsorbed molecules leads to their subsequent chemical activation at higher temperatures after the displacement of atoms of the adsorbed molecule corresponding to the most intense low-frequency infrared band [42]. Thus, the initially proposed structure for the product of C–H activation of ethane on GaH Z_d was built by displacement of the H1 atom by 1 Å in structure **IV** following the aforementioned C–H stretching vibration. Geometry optimization of the resulting structure leads to formation of product **VI** of the "alkyl" heterolytic C–H bond cleavage. The calculated activation energy for this process [**IV** → **VI**; Fig. 4, route (b)] is equal to 104 kJ/mol. The corresponding transition state structure **TS6** is characterized by an increase in the "alkyl" C1–H1 bond polarization, resulting in formation of a proton (H^+) attached to the basic zeolitic O atom and an alkyl ($C_2H_5{}^-$) grafted to the gallium ion. The resulting product, **VI**, is destabilized due to localization of likely charged ions (H^+ and $[H–Ga–C_2H_5]^+$) in the immediate vicinity of one another. However, it can be further stabilized by 195 kJ/mol via proton transfer from O4 (structure **IV**) to the more basic O7 ion bounded to the Al2 (structure **II**). It was shown previously [34] that the activation energy of this process does not exceed 50 kJ/mol.

It was also found that the product (**V**) of "carbenium" activation of C_2H_6 on GaH Z_d is just 14 kJ/mol less stable than structure **VI** [Fig. 4 routes (a) and (b), respectively]. Unfortunately, we could not locate the transition-state structure corresponding to the "carbenium" mechanism of ethane activation on GaH^{+2} species [**IV** → **V**; Fig. 4, route (a)] proposed by Joshi and Thomson [22]. However, with regard to the above discussion, it is obvious that this process will be less favorable than the "alkyl" one, because reaction **IV** → **V** requires very strong "repolarization" of the electron density of adsorbed ethane to produce a negative charge on H1 and a positive charge on the carbon atom (C1). There do not appear to be any facilitating factors for this process, and hence we surmise that the "carbenium" pathway will be strongly disfavored in comparison with the "alkyl" activation of ethane on charge-compensating GaH^{+2} sites.

Thus, the initial activation of C_2H_6 on GaH Z_d results in formation of the intermediate **II**, and hence, the catalytic cycle follows the reaction pathway described for ethane dehydrogenation over Ga Z_d (Section 3.2), and GaH^{+2} is converted to Ga^+.

3.5. *Effect of Al–Al distance on the reactivity of Ga^+ and GaH^{+2} sites*

The stability and reactivity of Ga^+ and GaH^{+2} ions in the Z_s cluster model were compared with those for clusters in which aluminum atoms are separated by a relatively long distance (8.138 Å). Here we present the computational results of ethane activation over these ions compensating for the negative charge in cluster models in which the aluminum ions are placed at the next-nearest allowed framework positions [Ga Z_s and GaH Z_s; r(Al1–Al2) = 4.837 Å]. The intermediates and transition-state structures thus calculated are very similar to those obtained for the Z_d model and exhibit similar trends in changes of geometry and charge parameters of intermediates due to chemical conversions. The calculated energetic parameters for elementary steps of ethane activation on Ga Z_s and GaH Z_s are summarized in Table 5.

The activation energies and enthalpies for both the homolytic and heterolytic C–H bond cleavage on Ga^+ ion in Z_s clusters are very similar to those calculated for the distantly separated Al atoms. Thus, it can be concluded that relative localization of anionic $[AlO_2]^-$ units in the framework of zeolite does not significantly affect the reactivity of the charge-compensating univalent gallium ions. In contrast, the chemical properties of GaH^{+2} depend strongly on the Al–Al distance in the cluster used. Similar to Joshi and Thomson [22], we could not detect activated molecular adsorption of ethane on GaH Z_s corresponding to the earlier-considered structure **IV** (Fig. 4). This is most likely connected to the fact that GaH^{+2} ion is much more strongly coordinated with the basic lattice oxygens of Z_s than with those of Z_d cluster model. Hence, coordination of ethane with the low-coordinated gallium ion cannot even partially compensate for the loss of energy due to Ga–O bond breaking, which is necessary for the formation of the $C_2H_6\ldots GaH^{+2}$ activated adsorption complex. This agrees well with a much higher activation barrier for the "alkyl" C–H bond dissociation. As follows from Table 5, the energy cost of the re-

action (4) is 42 kJ/mol higher in the GaH Z_s site than in the GaH Z_d site,

$$Z^-GaH^{+2}Z^- + C_2H_6 \rightarrow [H\text{–}Ga\text{–}C_2H_5]^+Z^- + H^+Z^- . \quad (4)$$

The transition-state structure for the "carbenium" initial activation of ethane on GaH Z_s was not identified. However, the enthalpy of this process is equal to +274 kJ/mol; therefore, the activation energy would be expected to be higher than this value. This then significantly exceeds the value of the activation energy calculated for the "alkyl" pathway. Taking into account the results of Section 3.4, the latter process seems to be more favorable over GaH^{+2} ions independent of the distance between charge-compensating $[AlO_2]^-$ anionic sites.

4. Discussion

In the present study, we considered three possible types of charge-compensating gallium species in reduced Ga/ZSM-5: Ga^+, $GaH_2{}^+$, and GaH^{+2}. Stability of univalent species (Ga^+, $GaH_2{}^+$) is remarkably higher than that of GaH^{+2} in the case of low Al content in zeolite, that is, distantly separated framework Al atoms. In contrast, when the Al–Al distance is rather small (with two aluminums located in the next-nearest positions), the presence of bivalent ions is preferred in the immediate vicinity of two anionic sites. The repulsive interaction between two closely situated positively charged univalent species results in strong destabilization of Ga^+ and $GaH_2{}^+$ at such cation sites.

The fraction of cation sites containing two aluminum atoms in the next-nearest positions is small; for instance, in a zeolite with an Si:Al ratio of 25, it does not exceed 30% [43]. Thus, with regard to the results presented in Table 1, it can be concluded that univalent Ga^+ or $GaH_2{}^+$ ions are the predominant charge-compensating species in high-silica gallium-exchanged zeolites, whereas GaH^{+2} cations can be found in only a relatively small portion of zeolitic cation sites, which contain two Al atoms.

It was found that at the initial step of ethane activation, all of the gallium species considered act as Lewis acids promoting heterolytic C–H cleavage involving the basic oxygen atoms of the zeolite lattice. In Ga^+ and $GaH_2{}^+$ active sites, this results in the formation of very unstable neutral Ga–C_2H_5 and H_2Ga–C_2H_5 species, respectively, as well as a Brønsted acid site, which readily either oxidizes Ga–C_2H_5 species or recombines with one of the hydride ions bounded to H_2Ga–C_2H_5, leading to desorption of hydrogen. In both cases, at the end of the reaction, very stable $[H\text{–}Ga\text{–}C_2H_5]^+Z^-$ species (**II**) are formed.

The catalytic cycle is closed by one-step decomposition of $[H\text{–}Ga\text{–}C_2H_5]^+Z^-$. It was found that simultaneous desorption of H_2 and C_2H_4 from these species [reaction (5)] is the most favorable process. The activation energy for production of Ga^+ from $[H\text{–}Ga\text{–}C_2H_5]^+$ following reaction (5) is 33 kJ/mol lower than that for regeneration of $GaH_2{}^+$ via desorption of ethylene (6). Moreover, under the conditions of the catalytic process, due to the entropy factor, the ΔG°_{823} is much lower for reaction (5) than for reaction (6) (−74 vs. +1 kJ/mol),

$$[H\text{–}Ga\text{–}C_2H_5]^+Z^- \rightarrow Ga^+Z^- + C_2H_4 + H_2 \quad (5)$$

and

$$[H\text{–}Ga\text{–}C_2H_5]^+Z^- \rightarrow GaH_2{}^+Z^- + C_2H_4. \quad (6)$$

Indeed, in reaction (5), rotation of the ethyl group results in formation of some weak attractive interaction between an unlikely charged hydride ion and a H atom from the β-methyl group of the $C_2H_5{}^-$ bound to gallium. In contrast, reaction (6) proceeds via abstraction of a hydride ion by a positively charged gallium from the same β-methyl group. This process requires significant repolarization of the C–H bond involved and thus exhibits a higher activation barrier. Therefore, ethane dehydrogenation over dihydrido-gallyl ions results in their decomposition. The equilibrium concentration of $GaH_2{}^+$ at high temperature is very low, and hence these sites cannot be considered responsible for ethane dehydrogenation. This finding is in agreement with the recent experimental results [16] indicating decomposition of $GaH_2{}^+$ ions in the catalytic process.

According to the results presented above on the reactivity of GaH^{+2} species, these species do not play a significant role as active sites in the reaction considered. In addition, the mechanism of ethane activation proposed by Joshi and Thomson [22] is disputable. Those authors suggested that gallium in such species acts as a hydride ion acceptor and that the C–H bond polarization follows a "carbenium" mechanism ($C^{\delta+}$–$H^{\delta-}$); however, the activated molecular adsorption of ethane, which precedes C–H cleavage, results in the opposite $C^{\delta-}$–$H^{\delta+}$ polarization. Note that this finding is in line with the higher electronegativity of carbon with respect to hydrogen (2.5 vs. 2.1 in the Pauling scale [44]). It is obvious that subsequent dissociative adsorption of ethane should follow the "alkyl" mechanism leading to formation of the intermediate product $[H\text{–}Ga\text{–}C_2H_5]^+Z^-$.

It is also noticeable that the GaH^{+2} species are isolobal to Zn^{+2} ions. This is reflected in the similarities of both the geometry and the charge properties of the zeolitic cation sites containing corresponding species (Table 1), as well as their chemical properties. Recently, it was shown experimentally [42,45] and theoretically [41] that the "alkyl" pathway of hydrocarbon dehydrogenation over zinc-exchanged zeolites is much more favorable than the "carbenium" pathway. The same conclusion follows directly from the calculations presented for GaH^{+2} ions exchanged in zeolite independently on the distance between charge-compensating $[AlO_2]^-$ framework units. The reactivity of either Ga^+ or $GaH_2{}^+$ in hydrocarbon activation exhibits very slight dependence on the distribution of aluminum in zeolite. In contrast, the GaH^{+2} stabilized in the cation site containing two anionic sites in the same zeolitic ring is much less active than that in the "charge-alternating" cation site.

Summarizing the foregoing results, we can conclude that univalent Ga^+ ions at cation sites of high-silica zeolites are the most probable active species for the hydrocarbon dehydrogenation reaction. The apparent activation barrier for this process estimated within the model used is equal to 233 kJ/mol. To the best of our knowledge, no experimental data are available on the activation energies for alkane dehydrogenation over well-defined gallium-exchanged zeolites. However, the apparent activation barrier estimated for ethane dehydrogenation over

Ga_2O_3/HZSM-5 [46] is significantly lower (163 kJ/mol) than this value. This disagreement is most likely due to the imperfection of the model used. Indeed, it does not take into account the electrostatic field of the zeolite cage, which can significantly stabilize polar transition state structures [47] involved in this process. Moreover, physical adsorption of ethane (∼20–30 kJ/mol) due to dispersive interactions between the hydrocarbon molecule and zeolitic walls, which cannot be correctly estimated by DFT, also decreases apparent activation energy compared with the true one.

5. Conclusion

The reaction mechanism of ethane dehydrogenation was investigated using DFT calculations for various reduced-gallium sites in Ga/ZSM-5. The probable catalytic cycle starts with the heterolytic C–H bond cleavage involving exchanged univalent gallium cation and a basic oxygen atom of the zeolite framework. The low energy of the d-orbitals of Ga^+ and its occupied s-orbital that make them unable to donate or accept electrons, respectively, from the hydrocarbon result in a high barrier for the direct oxidative addition of ethane to the cation. Therefore, heterolytic splitting of the C–H bond is much more favorable due to the polarization induced by the interaction of the hydrocarbon with the Ga…O Lewis acid–base pair. The resulting product easily rearranges to form $[H–Ga–C_2H_5]^+$, which decomposes via simultaneous desorption of H_2 and C_2H_4, regenerating the initial Ga^+ species. The overall activation barrier for C_2H_6 dehydrogenation over Ga^+Z^- sites is equal to 233 kJ/mol.

Hydrogenated gallium species ($GaH_2{}^+Z^-$ and $Z^-GaH^{+2}Z^-$) are less likely active sites. Decomposition of the dihydridogallyl ions, resulting in formation of univalent gallium ions during the catalytic cycle, is significantly favored over regeneration of $GaH_2{}^+$ sites. In addition, the estimated overall activation barrier for the considered catalytic reaction is higher (by 58 kJ/mol) for $GaH_2{}^+$ sites than for Ga^+ sites.

Bivalent GaH^{+2} species stabilized at the cation site with distantly separated framework Al sites exhibit significantly higher initial activity for ethane activation but much lower stability compared with Ga^+ sites. However, initial heterolytic cleavage of the C–H bond results in formation of $[H–Ga–C_2H_5]^+$ ions that preferentially follow the reaction path, again leading to univalent gallium cations.

On the other hand, GaH^{+2} ions charge-compensating two proximate framework aluminum ions are the most stable cationic species; however, initial activation of the C–H bond over these sites is strongly disfavored both thermodynamically and kinetically. In contrast, the reactivity of univalent gallium species exchanged in zeolite depends only slightly on the relative position of zeolitic anionic sites ($[AlO_2]^-$ units).

Acknowledgments

The authors thank Professor G.M. Zhidomirov for fruitful discussions. This work was sponsored by the National Computing Facilities Foundation, which provided supercomputer facilities, with financial support from the Netherlands Organization for Scientific Research (NWO). Support from the Dutch Science Foundation in the collaborative Russian–Dutch research project 047-015-001 NWO is also acknowledged.

References

[1] Hagen, F. Roessner, Catal. Rev. 42 (2000) 403.
[2] H. Kitagawa, Y. Senoda, Y. Ono, J. Catal. 101 (1989) 72.
[3] N.S. Gnep, J.Y. Doyemet, M. Guisnet, J. Mol. Catal. 45 (1988) 281.
[4] G.L. Price, V. Kanazirev, J. Catal. 126 (1990) 267.
[5] G.L. Price, V. Kanazyrev, K.M. Dooley, V.I. Hart, J. Catal. 173 (1998) 17.
[6] B.S. Kwak, W.M.H. Sachtler, W.O. Haag, J. Catal. 149 (1994) 465.
[7] B.S. Kwak, W.M.H. Sachtler, J. Catal. 145 (1994) 456.
[8] J. Yao, R. le van Mao, L. Dufresne, Appl. Catal. A: Gen. 65 (1990) 175.
[9] E. Iglesia, J.E. Baumgartner, G.L. Price, J. Catal. 134 (1992) 549.
[10] E. Iglesia, J.E. Baumgartner, Catal. Lett. 21 (1993) 55.
[11] G.D. Meitzner, E. Iglesia, J.E. Baumgartner, E.S. Huang, J. Catal. 140 (1993) 209.
[12] J.A. Biscardi, E. Iglesia, Catal. Today 31 (1996) 207.
[13] E. Iglesia, D.G. Barton, J.A. Biscardi, M.J.L. Gines, S.L. Soled, Catal. Today 38 (1997) 339.
[14] V.B. Kazansky, I.R. Subbotina, N. Rane, R.A. van Santen, E.J.M. Hensen, Phys. Chem. Chem. Phys. 7 (2005) 3088.
[15] V.B. Kazansky, I.R. Subbotina, R.A. van Santen, E.J.M. Hensen, J. Catal. 227 (2004) 263.
[16] N. Rane, A.R. Overweg, V.B. Kazansky, R.A. van Santen, E.J.M. Hensen, J. Catal., accepted for publication.
[17] M.V. Frash, R.A. van Santen, J. Phys. Chem. A 104 (2000) 2468.
[18] N.O. Gonzales, A.K. Chakraborty, A.T. Bell, Top. Catal. 9 (1999) 207.
[19] H. Himei, M. Yamadaya, M. Kubo, R. Vetrievel, E. Broclawik, A. Miyamoto, J. Phys. Chem. 99 (1995) 12461.
[20] E. Broclawik, H. Himei, M. Yamadaya, M. Kubo, A. Miyamoto, R. Vetrievel, J. Chem. Phys. 103 (1995) 2102.
[21] M.S. Pereira, M.A.C. Nascimento, Chem. Phys. Lett. 406 (2005) 446.
[22] Y.V. Joshi, K.T. Thomson, Catal. Today 105 (2005) 106.
[23] S. Kaliaguine, G. Lemay, A. Adnot, S. Burelle, R. Audet, G. Jean, J.A. Sawicki, Zeolites 10 (1990) 559.
[24] E.J.M. Hensen, M. Garcia-Sanchez, N. Rane, P.C.M.M. Magusin, P. Liu, K. Chao, R.A. van Santen, Catal. Lett. 101 (2005) 79.
[25] M. Garcia-Sanchez, P.C.M.M. Magusin, E.J.M. Hensen, P.C. Thüne, X. Rozanska, R.A. van Santen, J. Catal. 219 (2003) 352.
[26] V.B. Kazansky, I.R. Subbotina, R.A. van Santen, E.J.M. Hensen, J. Catal. 233 (2005) 351.
[27] H. Lermer, M. Draeger, J. Steffen, K.K. Unger, Zeolites 5 (1985) 131.
[28] D.H. Olson, G.T. Kokotailo, S.L. Lawton, W.M. Meier, J. Chem. Phys. 85 (1981) 2238.
[29] A.D. Becke, Phys. Rev. A 38 (1988) 3098;
A.D. Becke, J. Chem. Phys. 98 (1993) 1372;
A.D. Becke, J. Chem. Phys. 98 (1993) 5648.
[30] J. Backer, M. Muir, J. Andzelm, A. Scheiner, in: B.B. Laird, R.B. Ross, T. Ziegler (Eds.), Chemical Applications of Density-Functional Theory, ACS Symposium Series, vol. 629, American Chemical Society, Washington, DC, 1996.
[31] M.J. Frisch, G.W. Trucks, H.B. Schlegel, G.E. Scuseria, M.A. Robb, J.R. Cheeseman, J.A. Montgomery, Jr., T. Vreven, K.N. Kudin, J.C. Burant, J.M. Millam, S.S. Iyengar, J. Tomasi, V. Barone, B. Mennucci, M. Cossi, G. Scalmani, N. Rega, G.A. Petersson, H. Nakatsuji, M. Hada, M. Ehara, K. Toyota, R. Fukuda, J. Hasegawa, M. Ishida, T. Nakajima, Y. Honda, O. Kitao, H. Nakai, M. Klene, X. Li, J.E. Knox, H.P. Hratchian, J.B. Cross, C. Adamo, J. Jaramillo, R. Gomperts, R.E. Stratmann, O. Yazyev, A.J. Austin, R. Cammi, C. Pomelli, J.W. Ochterski, P.Y. Ayala, K. Morokuma, G.A. Voth, P. Salvador, J.J. Dannenberg, V.G. Zakrzewski, S. Dapprich, A.D. Daniels, M.C. Strain, O. Farkas, D.K. Malick, A.D. Rabuck, K. Raghavachari, J.B. Foresman, J.V. Ortiz, Q. Cui, A.G. Baboul, S. Clifford, J. Cioslowski, B.B. Stefanov, G. Liu, A. Liashenko, P. Piskorz, I. Komaromi, R.L. Martin, D.J. Fox, T. Keith, M.A. Al-Laham, C.Y. Peng, A.

Nanayakkara, M. Challacombe, P.M.W. Gill, B. Johnson, W. Chen, M.W. Wong, C. Gonzalez, J.A. Pople, Gaussian 03 (Revision B.05), Gaussian, Inc., Pittsburgh PA, 2003.
[32] G.M. Zhidomirov, A.A. Shubin, V.B. Kazansky, R.A. van Santen, Theor. Chem. Acc. 114 (2005) 90.
[33] G.M. Zhidomirov, A.A. Shubin, V.B. Kazansky, R.A. van Santen, Int. J. Quantum Chem. 100 (2004) 489.
[34] A.A. Shubin, G.M. Zhidomirov, V.B. Kazansky, R.A. van Santen, Catal. Lett. 90 (2003) 137.
[35] A.A. Shubin, G.M. Zhidomirov, A.L. Yakovlev, R.A. van Santen, J. Phys. Chem. B 105 (2001) 4928.
[36] P.Y. Bruice, Organic Chemistry, 2nd ed., Prentic-Hall, New Jersey, 1998.
[37] C.H. Hall, R.N. Perutz, Chem. Rev. 96 (1996) 3125.
[38] W.D. Jones, Acc. Chem. Res. 36 (2003) 140.
[39] S. Niu, M.B. Hall, Chem. Rev. 100 (2000) 353.
[40] G. Wilkinson, R.D. Gillard, J.A. McCleverty (Eds.), Comprehensive Coordination Chemistry, vol. 3, Pergamon Press, Oxford, 1987, p. 1601.
[41] M.V. Frash, R.A. van Santen, Phys. Chem. Chem. Phys. 2 (2000) 1085.
[42] V.B. Kazansky, E.A. Pidko, J. Phys. Chem. B 109 (2005) 2103.
[43] Y. Kuroda, R. Kumashiro, A. Itadani, M. Nagao, H. Kobayachi, Phys. Chem. Chem. Phys. 3 (2001) 1383.
[44] C.S.G. Philips, R.J.P. Williams, Inorganic Chemistry, Oxford University Press, Oxford, 1965, p. 114.
[45] V.B. Kazansky, A.I. Serykh, E.A. Pidko, J. Catal. 225 (2004) 369.
[46] J. Bandiera, Y.B. Taarit, Appl. Catal. A 152 (1997) 43.
[47] X. Rozanska, R.A. van Santen, in: C.R.A. Catlow, R.A. van Santen, B. Smith (Eds.), Computer Modelling of Microporous Materials, Elsevier, Amsterdam, 2004, p. 287.